

MICROSTRUCTURAL ANALYSIS OF SHOCKED APATITE FROM THE PAASSELKÄ IMPACT STRUCTURE, FINLAND

Gavin G. Kenny

Department of Geosciences, Swedish Museum of Natural History, SE-104 05 Stockholm, Sweden.

(gkenny@ gmail.com)

Introduction: Apatite, $\text{Ca}_5(\text{PO}_4)_3(\text{F},\text{Cl},\text{OH})$, is an almost ubiquitous accessory mineral that forms in igneous, metamorphic, sedimentary, hydrothermal and biological environments on Earth, as well as a range of settings on other planetary bodies. It is widely applied in geochronology and thermochronology [e.g., 1] and has been a particularly powerful tool in tracing abundance of, and processes related to, water and other volatiles in the inner Solar System [e.g., 2]. However, despite this, we know relatively little about how this mineral responds to the extreme temperatures and pressures associated with impact cratering.

In recent years, microstructural analysis of minerals such as zircon [e.g., 3-4], monazite [e.g., 5-6], baddeleyite [e.g., 7] and titanite [e.g., 8-9] have transformed our understanding of shock deformation in these phases. However, despite increasing use of apatite in dating of terrestrial impact structures [e.g., 10-11], microstructural analysis of the mineral has not been widely applied. Recently, electron backscatter diffraction (EBSD) microstructural analysis has been applied to lunar apatite [12] and here this is built upon with the first such study of terrestrial apatite.

Sample: A cobble of clast-rich impact melt rock from the ~10 km-in-diameter Paasselkä impact structure, Finland, was investigated. The allochthonous sample was recovered from the Sikosärkät till pit near the southeastern shore of the lake filling the structure.

Methods: Apatite grains were separated from the sample of clast-rich impact melt rock by crushing the rock in a jaw crusher and milling the resulting chips in a ring-and-puck-style mill. The heavy minerals were concentrated by magnetic separation with a hand magnet and Frantz magnetic separator, and heavy liquid density separation using methylene iodide diluted to a density of approximately 3.1 g/cm^3 . Eight apatite grains were identified and mounted on sticky carbon tabs so that their exteriors could be imaged in backscattered electron (BSE) mode on an FEI Quanta FEG 650 scanning electron microscope (SEM) at the Swedish Museum of Natural History, Stockholm. After external imaging, the grains were mounted in epoxy and polished in order to expose their mid-sections. A final polish with colloidal silica prepared the grains for microstructural analysis. Imaging and microstructural analyses by EBSD were then carried out on the interior surfaces on the same SEM.

Given the lack of a single established match unit for apatite, a range of match units were made in the Twist module of Oxford Instruments' HKL Channel 5 software and trialed on the apatite grains from Paasselkä. Data for a range of fluorapatite compositions listed in the American Mineralogist crystal structure database (AMCSD) came from [13-21]. Apatite is generally considered to have the space group P63/m) but all hexagonal space groups were tested here.

Results: Imaging: Six of the seven apatite grains identified in the sample display granular recrystallization textures on their exteriors (e.g., Fig. 1A). However, granular textures are less readily visible on polished grain interiors and under the petrographic microscope.

EBSD: Microstructural analysis by EBSD reveals two distinct textures in the suite of grains: six of the seven grains are composed of euhedral, relatively strain-free granules which define individual domains that are generally aligned but locally subtly misoriented from each other (e.g., Fig. 1A-C) whereas the other grain appears to be composed of a single domain with up to 20° within-grain misorientation (Fig. 1D-F). Notably, one of the granular grains is only partially recrystallized, with EBSD analysis revealing an oval-shaped, non-granular region near the center of the grain.

Discussion: The first microstructural analysis of terrestrial shocked apatite has revealed a range of textures, including recrystallization and crystal-plastic deformation, which are similar to those previously observed in minerals such as zircon and monazite. It is particularly noteworthy that the striking recrystallization textures that were revealed by EBSD were often not visible with traditional imaging techniques, such as BSE imaging of polished grain interiors. In light of these findings, future work should integrate microstructural analysis, U-Pb dating and measurements of volatile abundances and isotopic compositions in apatite – both terrestrial and extra-terrestrial – that may have been exposed to hypervelocity impact.

Acknowledgements: Thanks to Martin Schmieder and Jarmo Moilanen for provision of the sample and Kerstin Lindén for support with sample preparation. Feedback from journal reviewers, including Timmons Erickson, was helpful in considering this dataset and is gratefully acknowledged. This work received funding from the European Union's Horizon 2020 research and innovation program under the Marie Skłodowska-Curie Individual Fellowship Grant Agreement No. 792030.

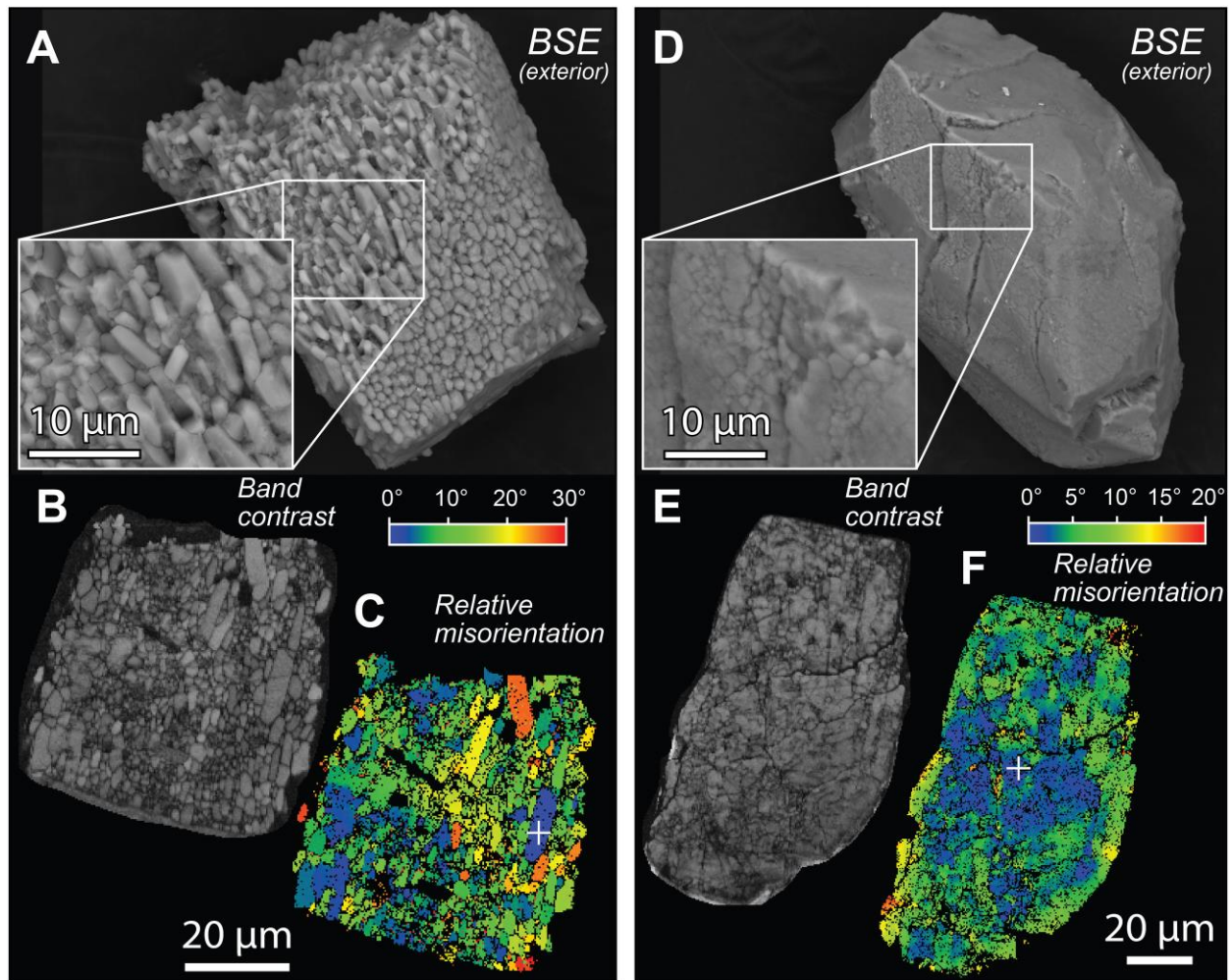


Fig. 1. Microstructural analysis of apatite grains from the Paasselkä impact structure, Finland, reveals recrystallization textures (left) as well as evidence for crystal-plastic deformation (right). A-C: Grain Paass-107ap (step size 300 nm); D-F: Grain Paass-106ap (step size 400 nm). BSE – backscattered electron.

References: [1] Chew, D. M. and Spikings, R. A. (2015) *Elements*, 11, 189–194. [2] McCubbin, F. M. and Jones, R. H. (2015) *Elements*, 11, 183–188. [3] Cavosie, A. J. et al. (2016) *Geology*, 44, 703–706. [4] Timms, N. E. et al. (2017) *Earth-Sci. Rev.*, 165, 185–202. [5] Erickson, T. M. et al. (2016) *Geology*, 44, 635–638. [6] Erickson, T. M. et al. (2017) *Contrib. Mineral. Petr.*, 172, 11. [7] White, L. F. et al. (2018) *Geology*, 46, 719–722. [8] Papapavlou, K. et al. (2018) *Contrib. Mineral. Petr.*, 173, 82. [9] Timms, N. E. et al. (2019) *Contrib. Mineral. Petr.*, 174, 38. [10] McGregor M. et al. (2018) *Earth Planet. Sci. Lett.*, 504, 185–197. [11] McGregor M. et al. (2019) *Contrib. Mineral. Petr.*, 174, 62. [12] Černok, A. et al. (2019) *Meteorit. Planet. Sci.*, 54, 1262–1282. [13] Hughes, J. M. et al. (1989) *Am. Mineral.*, 74, 870–876.

[14] Hughes, J. M. et al. (1990) *Am. Mineral.*, 75, 295–304. [15] Hughes, J. M. et al. (1991) *Am. Mineral.*, 76, 1165–1173. [16] Fleet, M. E. and Pan, Y. (1995) *Am. Mineral.*, 80, 329–335. [17] Rakovan, J. F. and Hughes, J. M. (2000) *Can. Mineral.*, 38, 839–845. [18] Comodi, P. et al. (2001) *Phys. Chem. Miner.*, 28, 219–224. [19] Hughes, J. M. et al. (2004) *Am. Mineral.*, 89, 629–632. [20] McCubbin, F. M. et al. (2008) *Am. Mineral.*, 93, 210–216. [21] Luo, Y. et al. (2009) *Am. Mineral.*, 94, 345–351.